Landau levels and edge states in carbon nanotubes: A semiclassical approach

P. Onorato

Department of Physics "A. Volta," University of Pavia, Via Bassi 6, I-27100 Pavia, Italy

(Received 18 May 2011; revised manuscript received 9 September 2011; published 6 December 2011)

The effects of a transverse magnetic field on the quantum mechanical magnetoelectronic structure of carbon nanotubes (CNs) are investigated, making use of the Einstein Brillouin Keller (EBK) semiclassical quantization. This approach, which is based on Dirac fermions moving on a cylindrical surface, gives detailed knowledge of the correspondence between the classical paths (cyclotron orbits localized at the top or the bottom of the CN, edge-skipping orbits restricted on the flanks of the tube, and traversing trajectories with charges rotating around the circumference) and the quantized EBK single-electron energies. The semiclassical approach also allows us to clearly distinguish within the magnetosubbands the geometrical effects of the curvature from the lattice effects and to estimate analytically the threshold field for the semiconducting-metallic transition in CNs.

DOI: 10.1103/PhysRevB.84.233403 PACS number(s): 61.48.De, 81.05.ue, 73.43.Lp, 03.65.Sq

Two-dimensional carbon compounds have recently attracted much attention due to the experimental observation in these materials of a number of novel electronic properties. Since its experimental isolation has become practicable,[1] it has been possible to measure the transport properties of a single layer of graphite (so-called graphene), providing evidence that the quasiparticles have a conical dispersion around discrete Fermi points.[2] Moreover, in the presence of a magnetic field perpendicular to the graphene plane, an unusual quantum Hall effect was discovered. These observations demonstrated that electrons can move through graphene with very low effective mass, exhibiting a behavior analogous to the transmission of relativistic massless particles.

Carbon nanotubes (CNs) can be considered as the result of wrapping up a graphene sheet, leading to systems with unconventional transport properties.[3] The electronic structure of CNs is closely related to the geometric structure, and single-wall CNs (SWCNs), which are obtained by wrapping up just a single layer of graphene, are predicted to be metallic or semiconducting depending on their radius and chiral angle.[3] The metallic CN and the graphene sheet have in common that their low-energy electronic dispersion mimics the physics of quantum electrodynamics and is governed by a Dirac equation for massless particles with spin around each of the two Fermi points of the undoped systems.[4] The appearance of an additional pseudospin quantum number intrinsic to the Dirac spectrum has allowed us to understand, for instance, the degeneracy of molecular orbitals in fullerenes[5] or the properties of the polarizability in CNs.[6] The presence of the (pseudo) spin degree of freedom due to the atomistic details of the carbon honeycomb lattice is responsible both for the insurgence of a gapless lowest Landau level in graphene and metallic CNs[7] and for the transition from the van Hove singularity pattern to the Landau level pattern at high magnetic field, which transforms a semiconducting CN into a metallic CN.[8]

In this paper, the effects of a transverse magnetic field on the magnetoelectronic band structure of CNs are investigated, making use of the description of the charge carriers as relativistic massless fermions with spin 1/2. This goal is pursued using the tools of semiclassical quantization,[9] namely, the Einstein Brillouin Keller (EBK) semiclassical quantization.[10] The latter quantization approach involves a path integral over the phase space of each coordinate q_i and its conjugate momentum p_i, given by

$$\left(n_i + \frac{\mu_i}{4}\right)\hbar = \frac{1}{2\pi}\oint p_i(q_i)dq_i + S_S, \tag{1}$$

where μ_i is the Maslov index, which is the total phase loss during one period in units of $\pi/2$. In detail, the Maslov index for a rotation is 0 and, for a libration, it is 2. With the aim of calculating the energies of particles with spin, an additive action S_S, which is due to the spin degree of freedom, is added in the EBK quantization rule when the particle undergoes a closed path. The latter action, calculated in Ref. 11 starting from the spin Lagrangian,[12] can be $S_S = \hbar/2$ or $S_S = 0$ according the trajectory. From this follows a general result obtained by Keppeler and coworkers[13] that, for relativistic fermions with spin 1/2, the Maslov phase and the spin contribution cancel each other when we consider a libration.

In CNs the effects of the geometrical curvature and those of the carbon lattice compete and produce a peculiar magnetoelectronic structure. Thus, in the remainder of the paper, the EBK electron energies in both a nanometric cylinder[9] and in a graphene layer[11] will be discussed as necessary grounds from which to calculate the magnetosubbands in CNs.

Since the classical and quantum motion of a spinless charged particle constrained to a curved surface and with a magnetic field applied is a nontrivial problem,[14] in Ref. 9 the electrons belonging to a cylindrical two-dimensional electron gas[15] were studied. In a cylindrical surface, different kinds of orbits are permitted as cyclotron orbits limited at the top or bottom of the tube surface, edge states localized on the flanks of the tube, and traversing trajectories corresponding to electrons which rotate around the tube. These classical trajectories were compared[9] with the one discussed for a plane quantum waveguide.[16] The explanation of Ref. 9 was based on an effective potential depending on the momentum of the charges along the cylinder's axis ($p_\perp \propto \kappa$) and including both the effects of the external field and the consequences of the geometrical curvature. Thanks to the semiclassical approach, a correspondence between the classical orbits and the energies was carried out analogously to what was shown for a planar system in Fig. 39 of Ref. 16. In momentum-energy space, (κ,ε), the different types of trajectories are separated by the two parabolas as in Fig. 5 of Ref. 9.

The low-energy electronic excitations in graphene obey a $(2+1)$-dimensional Dirac equation,[17] with holes and the sublattice state playing the role which positrons and spin play, respectively, in relativistic quantum mechanics.[18] Properly, the Dirac equation is a relativistic quantum mechanical equation which does not have a classical counterpart and which provides a description of elementary spin $1/2$ particles while graphene's Dirac equation, which follows from the tight binding (i.e., hopping) model, is

$$\mathcal{H}_{\mathcal{G}} = v_F(\sigma_x\pi_x + \sigma_y\pi_y), \tag{2}$$

where $v_F \simeq 1\times 10^6$ m/s is the Fermi velocity and π is the momentum measured from the Dirac points,

$$\pi_\alpha = \mathbf{p} - e\mathbf{A}(\mathbf{r})/c - \hbar\mathbf{K}_\alpha. \tag{3}$$

Here, α is the valley index ($\alpha = \pm$) labeling the two inequivalent points $\mathbf{K}_\pm$ in the Brillouin zone. According to the EBK action quantization for Dirac fermions,[11] the Hamiltonian $\mathcal{H}_{\mathcal{G}}$ can be simplified once one finds a constant of motion such as the spin along the direction of motion. The latter approach is equivalent to the so-called strong-coupling-limit (SCL) approximation used in several recent papers devoted to the semiclassical quantization of spinfull particles.[19] In the following, we use the SCL in order to denote the projection of spin along the direction of π.

In Ref. 11 the EBK action quantization was applied to obtain *Landau levels in plane graphene* and the *band structure of SWCNs*.

For the SCL and from the classical equations of motion for carriers in magnetic field, circular orbits were obtained with a cyclotron radius $R_c = v_F/\omega$, where $\omega = v_F^2 eB/(\varepsilon c)$ is the *relativistic cyclotron frequency* and ε is the particle energy.[11] Moreover, for cyclotron orbits in graphene, the spin precession during the period give a contribution to Eq. (1) of $S_S = \hbar/2$. Thus, the expression of the Landau levels as obtained in a fully quantum derivation[20] was recovered also by using EBK with $\varepsilon_n = \pm v_F\sqrt{2n\hbar eB}$. The presence of a zero-gap lowest Landau level for $n = 0$ explains the *anomalous quantum Hall effect* observed in graphene with the sequence of steps shifted by $1/2$ with respect to the standard sequence. Moreover, notice that the level spacing between adjacent Landau levels is not equally spaced since $\varepsilon_n \propto \sqrt{n}$ as is typical for relativistic particles (also spinless).

SWCNs are characterized by a roll-up wrapping vector, $\vec{w} = m_w\mathbf{a}_1 + n_w\mathbf{a}_2$, where n_w and m_w are integers (see Fig. 1). The CN's radius is $R = (|\vec{w}|)/(2\pi)$ and the momenta in Eq. (2) have to be taken along the circumference (π_w) and along the axis of the tube ($\pi_\perp$) by using a rotation of an angle θ where $\tan(\theta) = (m_w - n_w)/[\sqrt{3}(m_w + n_w)]$. It follows that $K_w = \{m_w - n_w\}/(3R)$ and $K_\perp = \{m_w + n_w\}/(\sqrt{3}R)$. From Eq. (2) in the SCL follows that $\varepsilon = v_F|\pi|$. Thus, once the energy ε is fixed, the result is

$$p_w(q_w,\varepsilon,\mathbf{K},p_\perp) = \sqrt{\varepsilon^2/v_F^2 - \pi_\perp^2} + \hbar K_w. \tag{4}$$

The EBK quantization along the wrapping direction is given by

$$\frac{1}{2\pi}\oint\sqrt{\frac{\varepsilon^2}{v_F^2} - \pi_\perp^2}\,dq_w + S_S - \oint K_w dq_w = \left(n + \frac{\mu_i}{4}\right)\hbar, \tag{5}$$

where $\mu_i = 0$ and $S_S = 0$ for rotations. From Eq. (5), ε is calculated and the semiclassical dispersion relation for massless Dirac fermions in a chiral CN is obtained as

$$\varepsilon_{m,p_\perp,\vec{w}} = v_F\hbar\sqrt{\frac{\delta^2}{R^2} + (k_\perp - K_\alpha)^2}, \tag{6}$$

where $\delta = \{3m - (m_w - n_w)\}/3$ and $p_\perp \equiv \hbar k_\perp$. Thus, a CN is considered metallic if the value $n_w - m_w$ is divisible by three. Otherwise, the CN is semiconducting.

Now we have to solve the semiclassical quantization equations for SWCNs in the presence of a magnetic field B (in the z direction); thus, the Landau gauge $\mathbf{A} = (A_w, A_\perp, A_z) = (0, Bx_w, 0)$ is chosen. We follow the same procedure reported in Ref. 9, where an effective potential was introduced. Here, $p_\perp$ is a constant of motion, and

$$V_{\text{eff}}(\varphi,\kappa_0) = \pi_\perp^2 = \Pi_0^2\,[\kappa_0 - \cos(\varphi)]^2\,,$$

where $\varphi \equiv q_w/R$, $\Pi_0 = Rm\omega_c$, and $\kappa_0 = (p_\perp - \hbar K_\perp)/(Rm\omega_c)$. The effective potential is analogous to that reported in the panels of Fig. 1 of Ref. 9 and an accurate analysis of $V_{\text{eff}}(\varphi,\kappa_0)$ allows a classification of the different trajectories reported in Figs. 1 and 2 of Ref. 9. EBK quantization rules, Eq. (5), provide the semiclassical quantized energies For transversing trajectories (rotations) $\oint K_w dq_w \neq 0$ and $S_S = 0$ while, both for cyclotron orbits and edge trajectories, $\oint K_w dq_w = 0$ and $S_S = \hbar/2$.

The classification of the different motions is now reported in Fig. 2 (top left), where the trajectories are represented in the energy-momentum space analogously to what was shown for a planar system in Fig. 39 of Ref. 16 and for a semiconducting tube in Fig. 5 of Ref. 9. The four straight lines divide the (κ_0,ε) plane into four regions which correspond to different types of trajectories, with cyclotron orbits localized at the top or bottom of the CN, edge-skipping orbits restricted to the flanks of the tube, and traversing trajectories with charges rotating around the circumference.

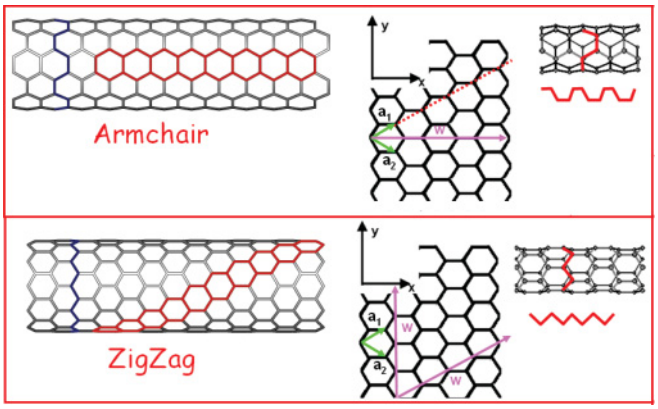

FIG. 1. (Color online) Structure of a SWNT can be conceptualized by wrapping a layer of graphene into a seamless cylinder. The way the graphene sheet is wrapped is represented by the chiral vector $\vec{w}$. The lattice vectors $\mathbf{a}_1 = a(\sqrt{3},1)/2$ and $\mathbf{a}_2 = a(\sqrt{3},-1)/2$ are shown. Here, $a_0 = a/\sqrt{3} \approx 1.42$ Å is the carbon-carbon distance and $\mathbf{K}_\pm \equiv (0,\pm 4\pi/(3a))$. In the case of the armchair CN (top panel), the vector $\vec{w}$ is $\vec{w} = (n,n)$, while the zigzag CN (bottom panel) is made by coiling a graphene sheet with a vector $(n,0)$ or $(n,-n)$.

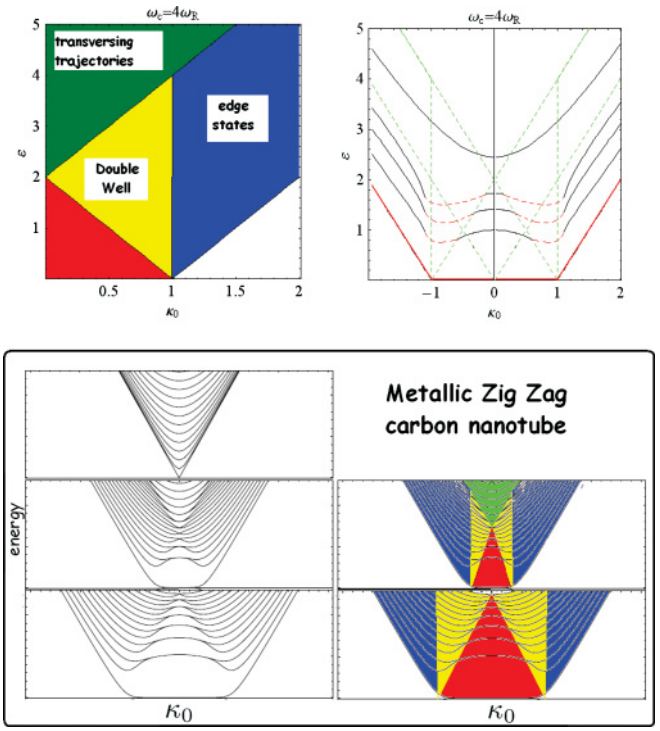

FIG. 2. (Color online) (top left) Energy-orbit phase space for a CN. Four regions correspond to different types of classical trajectories in a magnetic field: skipping orbits (edge states) and cyclotron orbits, where the electrons are confined in a single well $V_{\rm eff}$, traversing trajectories where the particle moves around the tube, and the region where the particle is confined in a double well $V_{\rm eff}$. The white region is forbidden. The region at the upper center contains transversing trajectories. (top right) The dispersion relation $\varepsilon_n(\kappa_0)$ for strong magnetic field obtained by using the EKB quantization and the harmonic expansion of $V_{\rm eff}$ near the minima. Notice that, as in Ref. 9 and also in CNs, the Landau level is not degenerate (i.e., for subbands with $n \geqslant 1$ the nondegenerate cyclotron orbits can be localized just at the top or at the bottom of the CN). In this case ($n \geqslant 1$), the anomalous reverse edge states are present with backward velocity, as discussed in Ref. 9. This is not more true for the lowest subband ($n = 0$), where a gapless, flat, and degenerate lowest Landau level exists for $|\kappa_0| < 1$ and while edge states dominate for $|\kappa_0| > 1$. Thus, for $n = 0$, cyclotron orbits are localized all over the CN's surface and exist for all the values of $|\kappa_0| < 1$. (bottom panel) Adapted from Ref. 21. Sequence of band structures of a metallic zigzag CN $\vec{w} = (510,0)$ in transverse magnetic field for $B = 0$ T, $B = 10$ T, and $B = 20$ T compared with theoretical phases predicted by using the semiclassical approach.

The latter orbits determine the dispersion relation $\varepsilon_n(\kappa_0)$ shown in Fig. 2 (top right). At the upper center, the typical parabolic behavior of transversing trajectories is reported. In the middle, the subbands coming from different kinds of orbits are presented: (i) the linear shape of the edge states, (ii) the nondegenerate Landau levels for $\kappa = 0$, and (iii) the reverse edge states for $\kappa_0 < 1$. At the bottom appears the special case of the lowest gapless subband, which has a sharp transition at $|\kappa_0| = 1$ from the cyclotron orbits (flat degenerate lowest Landau level) to edge states localized on the flanks. For large magnetic field strength, the energy levels at $\kappa_0 = 0$ follow the quantization rule $\varepsilon_n \propto \sqrt{n}$, which is peculiar to graphene.[20]

A comparison between semiclassical prediction about the energy orbit phase space and quantum results for the magnetic subbands obtained with a numerical tight-binding calculation is reported in the bottom panels of Fig. 2. The figure can be compared to what was shown for a planar system in Fig. 40 of Ref. 16.

As follows from Eq. (6), a semiconducting gap characterizes the band structure of two thirds of the CNs in the absence of a magnetic field. The semiconducting gap $\varepsilon_g = v_F\hbar\delta/R$ due to the CN's chirality is relevant just for the quantization of the transversing trajectories, where a rotation around the tube is allowed and $\oint K_w dq_w \neq 0$. Thus, when a magnetic field is switched on, a transition from semiconducting to metallic behavior happens. The lowest-energy transversing trajectory for $\kappa_0 = 0$ is allowed if $\varepsilon > V_{\rm eff}(0,0)$. Using the approximated value for $\varepsilon \sim v_F\hbar/\{R[\delta^2 + V_{\rm eff}(0,0)/2]^{1/2}\}$, we obtain a threshold field for the semiconducting-metallic transition:

$$B_t \sim \frac{c\hbar\sqrt{2}}{eR^2}\delta.$$

It follows that, for a CN with $R \sim 20$ nm, $[\vec{w} = (500,0)]$, such as the one discussed in Ref. 21, the threshold field is $B_t \sim 2$ T and is consistent with the results for semiconducting CNs from Ref. 22. From there we can infer that the magnetic field needed to close the gap of a CN with radius $R = 10$ nm must be of the order of $\sim$10 T. In agreement with Ref. 21, we obtained that the field strength B_t would be reduced by a factor of 4 after doubling the CN radius.

In this paper the effects of a transverse magnetic field on the electronic subband of CNs were investigated, making use of a long-wavelength description in terms of Dirac fermions. Thus, EBK semiclassical quantization, which includes the contribution of the spin degree of freedom, is adopted to deduce the quantum-mechanical energies.

The approach discussed allows a good understanding of the correspondence between the band structure and the trajectories of the charges along the tube by focusing on the following *strange* effects due to the curvature and those caused by the pseudospin:

(1) The interplay of the *curvature* and magnetic field causes the presence of different kinds of orbits: cyclotron orbits, edge orbits localized on the flanks of the tube, traversing trajectories, and anomalous edge orbits with backward velocity.

(2) The effects of the carbon lattice are due to the contribution of the *spin* action S_S and are emphasized by the presence of a gapless lowest Landau level.

(3) The level spacing between adjacent Landau levels is not equally spaced ($\varepsilon_n \propto \sqrt{n}$) as a consequences of the relativistic nature of carriers in graphene.

(4) Both the geometrical effect and the pseudospin contribution are responsible for the closure of the gap in a semiconducting CN at a threshold magnetic field proportional to the inverse square of the tube's radius, in agreement with the numerical results.

(5) Following Ref. 21, it is possible to calculate the Hall conductivity for a CN and to show that it is given by even multiples of $2e^2/h$. Thus, for thick CNs in a transverse magnetic field the transport properties are governed by the

states localized at the flanks of the CN (edge-skipping orbits), which carry quantized currents in the longitudinal direction.

From a theoretical point of view the approach presented here does not require the inclusion of the Berry topological phase in the calculation; in fact, the presence of the gapless lowest Landau level is explained just by applying the semiclassical quantization of Dirac fermions with spin, in agreement with the results obtained by Keppeler. This is a little different from the semiclassical approaches to graphene proposed in other previous works.[23,24]

From an experimental point of view, in some measurements it was shown that, when large-radius CNs (e.g., multiwall CNs) with a radius of the order of some tens of nanometers are examined, a magnetic field of tens of Tesla is sufficient to see relevant consequences.[25] We have to point out, however, that the results obtained herein describe the behavior of thick CNs—quite different from that of CNs with typical radii of 1 nm. In fact, for thin CNs in strong magnetic fields,[26] there is no regime where the continuum limit can be realized.

[1] K. S. Novoselov, A. K. Geim, S. V. Morozov, D. Jiang, Y. Zhang, S. V. Dubonos, I. V. Grigorieva, and A. A. Firsov, Science **306**, 666 (2004).

[2] K. S. Novoselov, A. K. Geim, S. V. Morozov, D. Jiang, M. I. Katsnelson, I. V. Grigorieva, S. V. Dubonos, and A. A. Firsov, Nature (London) **438**, 197 (2005).

[3] S. Bellucci and P. Onorato, in *Physical Properties of Ceramic and Carbon Nanoscale Structures*, The INFN Lectures–Lecture notes in Nanoscale Science and Technology, Vol. II, edited by S. Bellucci (Springer-Verlag, Berlin, Heidelberg, 2011).

[4] D. P. DiVincenzo and E. J. Mele, Phys. Rev. B **29**, 1685 (1984); J. González, F. Guinea, and M. A. H. Vozmediano, Nucl. Phys. B **406**, 771 (1993); C. L. Kane and E. J. Mele, Phys. Rev. Lett. **78**, 1932 (1997).

[5] J. González, F. Guinea, and M. A. H. Vozmediano, Phys. Rev. Lett. **69**, 172 (1992).

[6] D. S. Novikov and L. S. Levitov, Phys. Rev. Lett. **96**, 036402 (2006).

[7] N. M. R. Peres, F. Guinea, and A. H. Castro Neto, Phys. Rev. B **73**, 125411 (2006); V. P. Gusynin and S. G. Sharapov, Phys. Rev. Lett. **95**, 146801 (2005).

[8] S. Roche, G. Dresselhaus, M. S. Dresselhaus, and R. Saito, Phys. Rev. B **62**, 16092 (2000).

[9] S. Bellucci and P. Onorato, Phys. Rev. B **82**, 205305 (2010).

[10] A. Einstein, Verh. Dtsch. Phys. Ges. **19**, 82 (1917); L. Brillouin, J. Phys. Radium **7**, 353 (1926); L. J. Curtis and D. G. Ellis, Am. J. Phys. **72**, 1521 (2004); A. J. Larkoski, D. G. Ellis, and L. J. Curtis, *ibid.* **74**, 572 (2006).

[11] P. Onorato, Mod. Phys. Lett. B **25**, 537 (2011).

[12] M. Pletyukhov, Ch. Amann, M. Mehta, and M. Brack, Phys. Rev. Lett. **89**, 116601 (2002); A. Reynoso, G. Usaj, M. J. Sanchez, and C. A. Balseiro, Phys. Rev. B **70**, 235344 (2004).

[13] J. Bolte and S. Keppeler, Phys. Rev. Lett. **81**, 1987 (1998).

[14] G. Ferrari and G. Cuoghi, Phys. Rev. Lett. **100**, 230403 (2008).

[15] A. B. Vorob'ev, K.-J. Friedland, H. Kostial, R. Hey, U. Jahn, E. Wiebicke, J. S. Yukecheva, and V. Y. Prinz, Phys. Rev. B **75**, 205309 (2007); N. Shaji, H. Qin, R. Blick, L. Klein, C. Deneke, and O. Schmidt, Appl. Phys. Lett. **90**, 42101 (2007).

[16] C. W. J. Beenakker and H. van Houten, Solid State Phys. **44**, 1 (1991).

[17] D. P. DiVincenzo and E. J. Mele, Phys. Rev. B **29**, 1685 (1984); G. W. Semenoff, Phys. Rev. Lett. **53**, 2449 (1984).

[18] M. Mecklenburg and B. C. Regan, Phys. Rev. Lett. **106**, 116803 (2011).

[19] S. Bellucci and P. Onorato, Phisica E **42**, 1571 (2010).

[20] J. W. McClure, Phys. Rev. **104**, 666 (1956).

[21] E. Perfetto, J. Gonzalez, F. Guinea, S. Bellucci, and P. Onorato, Phys. Rev. B **76**, 125430 (2007); S. Bellucci, J. Gonzalez, F. Guinea, P. Onorato, and E. Perfetto, J. Phys. Condens. Matter **19**, 395017 (2007).

[22] J. P. Lu, Phys. Rev. Lett. **74**, 1123 (1995).

[23] P. Carmier and D. Ullmo, Phys. Rev. B **77**, 245413 (2008).

[24] P. Rakyta, A. Kormanyos, J. Cserti, and P. Koskinen, Phys. Rev. B **81**, 115411 (2010); A. Kormanyos, P. Rakyta, L. Oroszlany, and J. Cserti, *ibid.* **78**, 045430 (2008).

[25] U. Coskun, T.-C. Wei, S. Vishveshwara, P. Goldbart, and A. Bezryadin, Science **304**, 1132 (2004); S. Nanot, W. Escoffier, B. Lassagne, J.-M. Broto, and B. Raquet, Comptes Rendus Physique **10**, 268 (2009); B. Lassagne, J.-P. Cleuziou, W. Escoffier, R. Avriller, S. Roche, and L. Forro, Phys. Rev. Lett. **98**, 176802 (2007).

[26] R. Saito, G. Dresselhaus, and M. S. Dresselhaus, Phys. Rev. B **53**, 10408 (1996).